Citation: Dobrescu, A., 2021. Pre-Variscan granitoids with adakitic signature at west Getic basement of the South Carpathians (Romania): constraints on genesis and timing based on whole-rock and zircon geochemistry. Geologica Acta, 19.4, 1-17, I-II.
DOI: 10.1344/GeologicaActa2021.19.4

geologica acta

Pre-Variscan granitoids with adakitic signature at west Getic basement of the South Carpathians (Romania): constraints on genesis and timing based on whole-rock and zircon geochemistry

Anca Dobrescu

Department of Regional Geology, Geological Institute of Romania
Caransebes Str. 1, 012271, Bucharest 32, Romania
E-mail: ancadobrescu2003@yahoo.com

ABSTRACT

Research on two strata-like intrusions from Slatina-Timiş (STG) and Buchin (BG) at West Getic Domain of the South Carpathians (Semenic Mountains) identified granitoids with adakitic signature in a continental collision environment. Whole-rock geochemical composition with high Na_2O, Al_2O_3 and Sr, depleted Y (<18ppm) and HREE (Yb< 1.8ppm) contents, high Sr/Y (>40), $(La/Yb)_N$ (>10) ratios and no Eu anomalies overlaps the High-Silica Adakites (HSA) main characteristics, though there are differences related to lower Mg#, heavy metal contents and slightly increased $^{87}Sr/^{86}Sr$ ratios. Comparison with HSA, Tonalite-Trondhjemite-Granodiorite (TTG) rocks and melts from experiments on basaltic sources suggests partial melting at pressures exceeding 1.25GPa and temperatures of 800-900ºC (confirmed by calculated Ti-in zircon temperatures) as the main genetic process, leaving residues of garnet amphibolite, garnet granulite or eclogite type. The adakitic signature along with geochemical variations observed in the STG-BG rocks indicate oceanic source melts affected by increasing mantle influence and decreasing crustal input that may restrict the tectonic setting to slab melting during a subduction at low angle conditions. An alternative model relates the STG-BG magma genesis to garnet-amphibolite and eclogite partial melting due to decompression and heating at crustal depth of 60-50km during syn-subduction exhumation of eclogitized slab fragments and mantle cumulates. The granitoids were entrained into a buoyant mélange during collision and placed randomly between two continental units. U-Pb zircon ages obtained by LA-ICP-MS and interpreted as Ordovician igneous crystallization time and Variscan recrystallization imprint are confirmed by trace-element characteristics of the dated zircon zones, connecting the STG-BG magmatism to a pre-Variscan subduction-collision event. The rich zircon inheritance reveals Neoproterozoic juvenile source and older crustal components represented by Neoarchean to Paleoproterozoic zircons.

KEYWORDS **Granitoids; Adakitic signature; U-Pb zircon ages and geochemistry; Getic basement; Romanian South Carpathians.**

INTRODUCTION

Four Variscan granitoid plutons align from Serbia (in the South) to Romania (at North) as intrusions into the western Getic basement of the Alpine upper nappe in the South Carpathians. Small granitoids are randomly widespread among these plutons in the gneissic units of the Getic basement, some of them documented to be of Ordovician age (Balintoni *et al.,* 2010, 2014 and references therein). Two strata-like granitoid bodies at Slatina-Timiş (STG) and Buchin (BG) situated in the northeast part of the Semenic Mountains (Fig. 1) caught our attention by their particular geochemical characteristics and age related issues. They have adakitic signature: geochemical characteristics common to High-Silica Adakites (HSA) and Tonalite-Trondhjemite-Granodiorite (TTG) rocks, ground to search for their genesis and significance related to regional tectonic setting.

Since 1990s topics on HSA and TTG rocks have been constantly approached, concluding on their similarities sufficient to be regarded as analogues (Drummond and Defant, 1990; Martin, 1999), but also revealing differences (Martin *et al.*, 2005; Moyen and Martin, 2012). Their distinctive geochemical features (high Na_2O, Al_2O_3

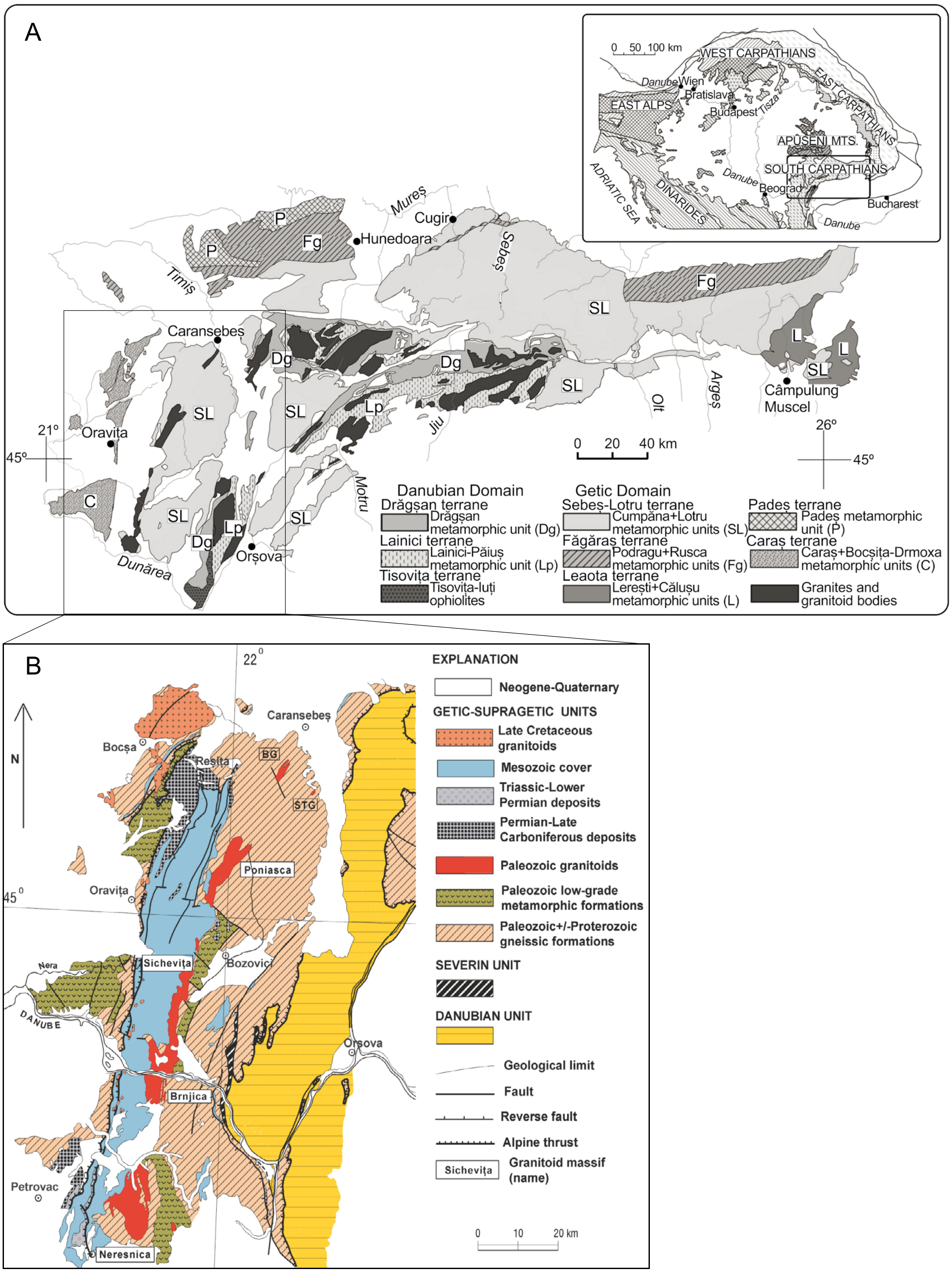

FIGURE 1. A) Geological map of Pre-Alpine terranes in the South Carpathians (Balintoni *et al.*, 2010 and references therein); B) STG and BG location at west South Carpathians (sketch map modified after Duchesne *et al.*, 2008; Iancu *et al.*, 2005; Săndulescu *et al.*, 1978).

(>15 %) and Sr (>400ppm), low HREE (Yb<1.9ppm) and Y (<18ppm) contents), more or less associated with high Sr/Y and La/Yb ratios, define the adakitic signature interpreted as derived from a basaltic source at pressures high enough to stabilize garnet ± amphibole (Atherton and Petford, 1993; Drummond and Defant, 1990). Experiments revealed that adakitic melts can be produced by partial melting of basaltic rocks at high pressure (≥1.0GPa), leaving a garnet + clinopyroxene ± amphibole ± plagioclase residue (Rapp and Watson, 1995). Studies on adakitic rocks established that they may form mainly related to slab melting in a subduction setting (Defant and Drummond, 1990; Drummond and Defant, 1990), although rocks with adakitic characteristics were also encountered in other tectonic settings, generated through different petrogenetic processes (Atherton and Petford, 1993; Defant and Drummond, 1990; Martin *et al.,* 2005; Moyen, 2009 and references therein). Some are associated to melting of mantle-derived materials underplated at the base of continental crust (Atherton and Petford, 1993), others to melting of delaminated garnet-bearing lower continental crust (Wang *et al.,* 2007) or to combined Assimilation and Fractional Crystallization (AFC) of mantle-derived magma during its transit through the continental crust (Castillo, 2006). Common to TTG rocks and few other types, the adakitic signature can reflect a range of situations and processes implying either melting of a high Sr/Y garnet-rich source, interaction with mantle in the garnet stability field or garnet-rich source fractionation (Moyen, 2009). Research of the last decades described many adakite-like rocks of low Heavy Rare Earth Elements (HREE) and Y contents, more or less associated with high Sr/Y and La/Yb ratios, aspects that are still a matter of debate due the variety of cases encountered.

The granitoids from Slatina-Timiş and Buchin are two of the rare cases of rocks with adakitic characteristics hosted in a continental collisional environment as the Getic basement of the Romanian Carpathian Mountains. They were studied in order to reveal the petrogenetic circumstances that generated their adakitic signature. The rocks were dated by in-situ U-Pb method on zircon crystals and interpreted as Ordovician intrusions (Dobrescu *et al.,* 2010). Due to the difficulty to date these granitoids on a limited number of crystals found and to the lack of information regarding the genetic significance of the dated growth zones, questions on the intrusion ages remained. Consequently, the accuracy of the age interpretation was verified by studying the trace- element behaviour in the dated zones. The relevance of the study lies in the ability of zircon to record petrogenetic processes in igneous and metamorphic systems (Hoskin and Schaltegger, 2003; Rubatto, 2002). As the whole-rock geochemical composition allowed only comparison and qualitative modeling on the main genetic process, sources and conditions, zircon trace-element behaviour was used to complete this information.

GEOLOGICAL BACKGROUND

The current tectonic models describe the South Carpathians as composed of three major units as a result of a thrust structure assembled during the Alpine collisional evolution. The lower continental Danubian Domain is a nappe system consisting of Neoproterozoic granites, metamorphic rocks and Paleozoic-Mesozoic sedimentary formations. The Severin oceanic crust is a tectonic mélange of Jurassic ophiolites, flysch and bimodal alkaline igneous rocks. The upper Getic Domain is composed of several pre-Alpine basement gneissic formations overlain by late Carboniferous to Permian sedimentary rocks and a transgressive late Cretaceous cover (Balintoni, 1997; Balintoni *et al.,* 2010; Iancu *et al.,* 2005; Medaris *et al.,* 2003; Săndulescu, 1984).

The Getic Domain basement was reconsidered, differently divided and renamed based on various litho-tectonic visions. Known as the Sebeş-Lotru pre-Alpine terrane, according to Balintoni *et al.* (2010) it comprises a lower Neoproterozoic metamorphic unit (Lotru) and an upper Ordovician metamorphic unit (Cump**ă**na) with rocks assemblages dominated by orthogneisses and metabasites, local paragneisses, quartzites and carbonate rocks; various sedimentary, volcanic, mafic and ultramafic protoliths were metamorphosed in medium-high grade conditions (Iancu and Mărunţiu, 1989). The two units were juxtaposed during the Variscan orogeny, sharing the foliation generated by the high-grade metamorphic event (Săbău and Massone, 2003) and the P-T signatures specific to the individual tectono-stratigraphic units (Medaris *et al.*, 2003). The same basement was renamed as Lotru Metamorphic Suite (LMS) and considered by Săbău (1999), Săbău and Massone (2003) as composed of three units. The uppermost Semenic Nappe (SN) consists of mica gneisses and schists; at its lower boundary, manganese silicate rocks, quartzites, tourmaline rocks, pegmatites and stratoid granitoids (like STG and BG) form a marker level called Delineşti, spatially associated with ultramafics, amphibolites and eclogites. The intermediate Voineasa Unit (VU) contains amphibolites, high grade gneisses (Valea Căprăreasa Complex: VCC) with eclogite inclusions and metagranitoids (Tilişca), a migmatized gneiss complex with eclogites and ultramafic lenses, a mafic terrigeneous complex and an alkaline meta-igneous complex. The lowermost Armeniş Unit (AU) consists of biotite-gneisses, leptynites, kinzigites, pegmatite segregation and a thin limestone body.

The Getic basement is intruded, at its western part, by four Variscan granitoid plutons (Neresnica and Brnjica in Serbia, Sicheviţa and Poniasca in Romania) interpreted to form a major batholith buried beneath the Mesozoic and Cenozoic cover (Duschesne *et al.,* 2008; Săndulescu *et al.,* 1978). Small granitoid bodies and migmatites are widespread in the gneissic units of the Getic basement (Balintoni, 1975; Iancu, 1998; related references in Iancu and Seghedi, 2018; Stelea, 2000), some of them documented as Ordovician (Balintoni *et al.,* 2010, 2014 and references therein). Two granitoid bodies outcrop in the Precambrian-lower Paleozoic medium-high grade Getic metamorphic basement: STG to the East and BG to the North-East from the Poniasca pluton (Fig. 1). Field observations (Gridan, 1981; Săbău, 1999; Savu, 1997) describe them as relating concordantly to the host rocks in the axial zone of two anticline structures, sometimes folded together or penetrating discordantly in places. According to Săbău (1999), the granitoids appear as strata-like laying on the gneisses of VU and beneath the micaschists of SN, although the relationship with the host rocks is complicated. Gridan (1981) and Savu (1997) described the rock mineralogy and petrography; Savu (1997) advanced a genetic model presuming a primary trondhjemitic magma resulted from a metasomatized mantle source controlled by subduction. Dimitrescu (2007) considered BG as a prolongation of the Variscan Poniasca pluton, while Conovici (2000) placed Poniasca, Sicheviţa and Beljanica plutons in a southern terrane with a distinct evolution from the northern terrane (where STG and BG occur).

The intrusions of STG and BG outcrop on areas of around 2km long by 0.6km wide and 12km long by 1.6km wide, respectively. The rocks are medium-fine grained, mostly with gneissic structure (Savu, 1997), described petrographically as tonalites and granodiorites in STG and granodiorites, trondhjemites and granites in BG samples. The STG mineralogy is composed of deformed quartz, zoned plagioclase (An_{15-27}), reddish-brown biotite and less greenish-brown biotite, rare microcline, accessory hornblende, zircon, zoned allanite, apatite, titanite, rutile, monazite and magnetite, secondary minerals like epidote, clinozoisite, muscovite, chlorite, iron oxides and pyrite. The BG rocks consist of deformed quartz, zoned plagioclase (An_{16-29}), green to greenish-brown biotite, microcline, hornblende and primary epidote, accessory titanite, rutile, zircon, apatite, rare muscovite, monazite, and secondary epidote, chlorite and opaque minerals. Aplites and rare pegmatites occur in the area; biotite-rich autholites and partly assimilated crystalline schists are concordantly disposed along margins. Contaminated rocks with biotite-almandine-muscovite-sillimanite association were observed at some margins (Savu, 1997). The two intrusions are locally crossed by fine leucocratic veins.

METHODS

Eighteen powdered bulk-rock samples were geochemically analyzed by X-Ray Fluorescence (XRF) and Inductively coupled plasma mass spectrometry (ICP-MS). Whole-rock samples were analyzed for major elements by a JY24 Sequential Spectrometer (ICP-AES), while Si was determined using a Spectro Analytical X-Lab 2000 XRF spectrometer. Detection limits for most elements were less than 0.005 wt.% in the sample and analytical errors characteristically varied from 2% to 5%, depending on the element determined and its concentration. Trace elements (including REE) were determined on totally digested samples ICP-MS using a VG Elemental Plasma Quad II. Precision varied from 5 to 10%, depending on the element determined and its concentration. All analyses were performed in the Department of Earth Sciences at the University of Bristol (UK). Analytical details for major and trace element measurements may be found in Marschall *et al.* (2005).

Rb-Sr isotope analyses needed isotope dilution, chemical separation, and mass spectrometer procedures performed at Prospecţiuni S.A. Laboratory, Bucharest (Romania). The isotope data were obtained using PS-LAG-CAFCH-RM-004 procedure on MI-1201T mass-spectrometer of solid-state ionization source and MIN-L and MIN-G international standards. $^{87}Sr/^{86}Sr$ ratios were corrected for fractionation using $^{86}Sr/^{88}Sr$= 0.1194. Analytical details and method are fully described in Bayanova *et al.* (2009).

In situ U/Pb zircon geochronology was performed using ELA-ICP-MS (Excimer Laser Ablation Inductively Coupled Plasma Mass Spectrometry) on 12 zircon crystals from a BG rock sample and on a single zircon from a STG rock sample (Table 1, see the Appendix). The zircon structure was examined by cathodoluminescence (CL) at University of Milan (Italy). U/Pb dating was carried out at CNR-Istituto di Geoscienze e Georisorse (Unita di Pavia) using an ArF excimer laser ablation microprobe operating at 193nm (Geolas200Q-Microlas) coupled with the High Resolution-ICP-MS (Element-Thermo Finnigan). Analytical details and method are fully described by Tiepolo (2003) and Dobrescu *et al.* (2010).

Geochemical analyses on the dated zircons were obtained by Secondary-Ion Mass Spectrometry (SIMS) using Cameca IMS-1280 ion microprobe at Nordsim facility in Stockholm which allows in situ measurements of isotopic and elemental composition in selected micrometer sized areas of polished sections. Trace-element contents of the zircon zones were analysed using the method described in Whitehouse *et al.* (1999) and Whitehouse and Kamber (2005).

RESULTS

Whole-rock geochemistry

The chemical composition of STG and BG samples is listed in Table I. STG rocks have 65.6-68.4wt.% SiO_2,

TABLE 1. Location of the dated samples

Sample	Rock type	Location	
BG	granitoid	Semenic Mts. - S Buchin village	N49^0 49' 18" E28^0 52' 30"
STG	granitoid	Semenic Mts. - Slatina-Timis valley	N49^0 42' 53" E28^0 57' 15"

high Al_2O_3 (16.5-17wt.%) and Na_2O (3.8-5.1wt.%), low-medium K_2O (1.4-3.8wt.%) contents and Na_2O/K_2O (1-3) ratios. BG rocks are more siliceous (67.7-73.6wt.% SiO_2) with higher Na_2O (4.6-6.4wt.%), K_2O (3.1-3.9wt.%) contents and Na_2O/K_2O ratios of (1.2-1.9). A/CNK values are of (0.99-1.26) for STG and (0.93-1.09) for BG (Fig. 2A). Trace-element behavior (Fig. 3A) shows Large Ion Lithophile Element (LILE) enrichment and depleted High Field Strength Elements (HFSE), with Nb-Ti negative anomalies. Medium-high Sr (554-966ppm), low Y (4-12ppm) and HREE (Yb of 0.38-1.23ppm) contents yield medium Sr/Y (48-87) and $(La/Yb)_N$ (9.75-39.9) ratios for STG and high Sr/Y (100-175) and medium $(La/Yb)_N$ (10.5-30.55) for BG. REE (Fig. 3B) show low to no Eu anomalies (Eu/Eu* of 0.79-1 for BG and 0.81-1.18 for STG). A range of Rb-Sr isotopic data has been obtained on 7 BG and 6 STG rock samples. The initial $^{87}Sr/^{86}Sr$ ratios were age-corrected at 464Ma (Dobrescu *et al.,* 2010) and vary between 0.7045-0.7051 for BG and 0.7042-0.7060 for STG (Table I).

Geochronology: age data review

Nineteen zircon U-Pb age data obtained by ELA-ICP-MS on STG and BG samples have been already published (Dobrescu *et al.,* 2010). The age data interpretation is revisited in this study in order to relate the different stages of zircon crystallization with tectono-thermal events that affected the Getic Domain basement.

The majority of the analyzed crystals has composite structures with inherited anhedral to subhedral cores surrounded by complex zoned overgrowths typical for deep-seated, slowly cooled granitic magmas and thinner outer rims; prismatic crystals with oscillatory zoning without inherited cores were also described (Fig. 4). The oldest inherited xenocrystic core is Neoarchean (2.5Ga) correlating with 2.4-2.6Ga ages encountered in orthogneisses and metagranites from the Sebeş-Lotru terrane (Balica, 2007) and with 2.5-2.7Ga detected in the upper low-grade Caraş terrane (petrographically similar to the Sebeş-Lotru terrane and presumed to have the same origin), interpreted as of Saharian provenance (Balintoni *et al.,* 2009). Corroded cores of Paleoproterozoic to lower Neoproterozoic ages (1878±57, 1857±56, 1055±39, 858±32Ma) are relicts contemporary to those detected by Balintoni *et al.* (2010) as detrital zircons in the upper Cumpăna unit, interpreted as of northeastern Gondwanan provenance. The Neoproterozoic age of 858Ma is close to the single inherited age (of 866Ma) evidenced in the Poniasca pluton (Duchesne *et al.,* 2008). Ages at 677±29, 600±22, 589±23 and 583±22Ma on well-developed concentric zoned cores are assigned to the main source for BG, contemporary with the Cadomian protoliths from the lower part of the Sebeş-Lotru terrane, with possible

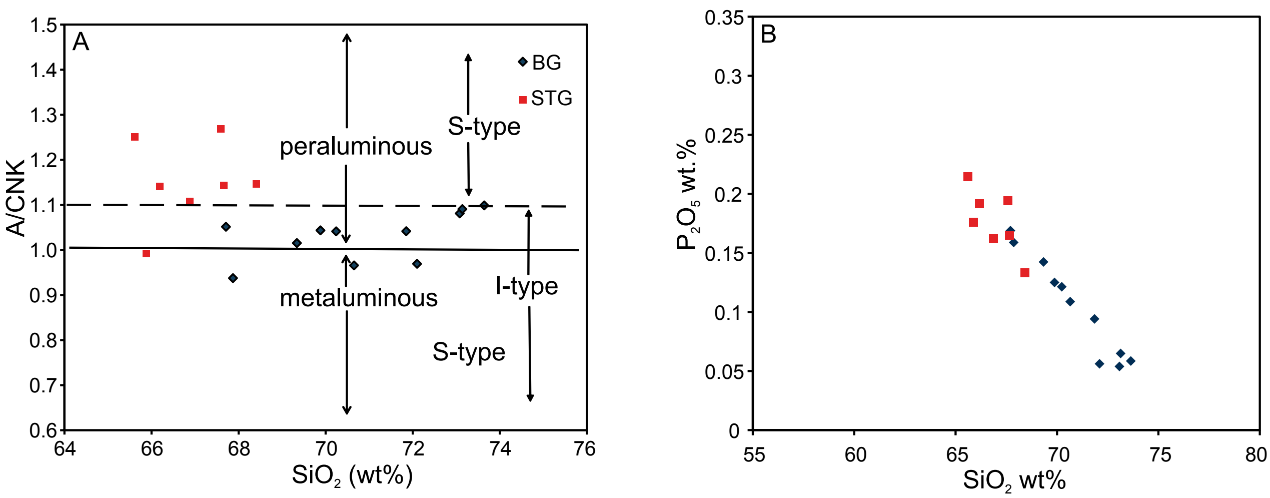

FIGURE 2. A) Rock/magma type classification for the STG-BG samples in A/CNK [molAl_2O_3/(CaO+Na_2O+K_2O)] vs. SiO_2 diagram (Chappel and White, 2001). B) Variation trends of STG and BG contents in P_2O_5 vs. SiO_2 diagram.

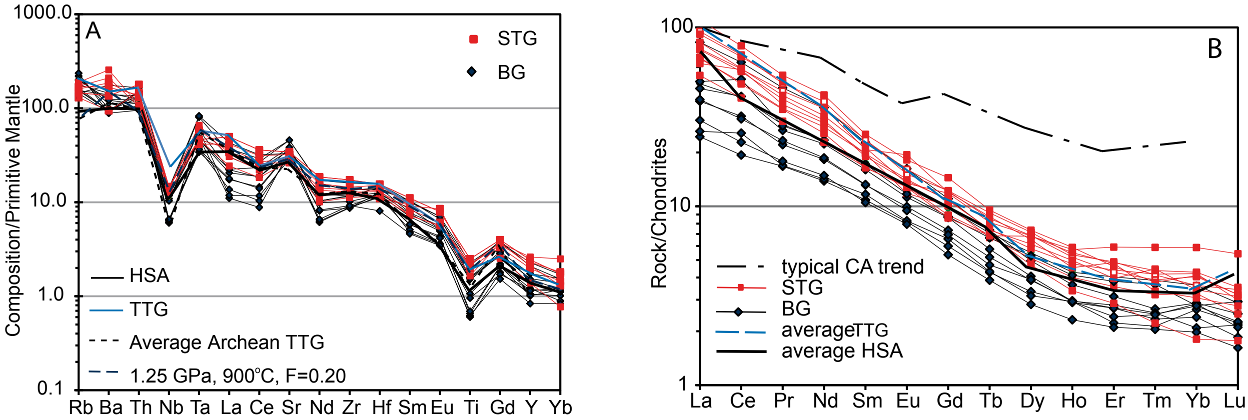

FIGURE 3. Multi-element diagrams for STG-BG samples: A) comparison with HSA and TTG trace-element contents in primitive-mantle normalized multi-element diagram; HSA and TTG from Martin *et al.* (2005); primitive mantle values from Sun and McDonough (1989); melts produced at 1.25GPa and 900ºC, F= 0.20 from RG2003, Rudnick and Gao (2003); B) chondrite-normalized REE diagram (normalizing coefficients from Boynton in Henderson (1984)); average TTG values from Drummond and Defant (1990); average HSA values from Moyen (2009); CA (calc-alkaline) trend of dacite REE from the Southern Volcanic Zone, Andes (Hickey-Vargas *et al.*, 1989).

Pan-African affinities (Balintoni *et al.,* 2009). Despite the limited number of dated crystals, the inherited BG zircons record the whole range of ages encountered in the Getic basement rocks (Balintoni *et al.,* 2014; Stoica *et al.,* 2016). The relicts are overgrown by Ordovician and Variscan zircon rims which imply that the inherited zircons were entrained at the source level. The ages of the oscillatory zoned overgrowths (a dominant feature of igneous zircons– Vavra, 1990) at 493±19 and 465±17Ma for STG and 462±18 and 434±19Ma for BG were interpreted as intrusion time-span, though data are relatively scattered and do not allow to unequivocally define an intrusion age. The four data yield a concordia age at 463.6±18Ma (1σ; MSWD= 0.04) (Dobrescu *et al.,* 2010) which makes STG and BG contemporary to several rocks belonging to the Cumpăna unit of the Sebeş-Lotru terrane (Căpâlna orthogneiss of 458.9Ma, Latoriţa orthogneiss of 466.0Ma) (Balintoni *et al.,* 2009, 2010, 2014) and to Tilişca granitoid (474-460Ma) (Săbău and Negulescu, 2012) which belongs to the VCC of the underlying VU. The ages coincide with a major pre-Variscan tectono-thermal event responsible for the incorporation of high-pressure rocks in the metamorphic complexes (Săbău and Massone, 2003). The dark-grey (low CL intensity) outer rims, some with "flow zones", convoluted zoning and transgressive recrystallization-seeming front more developed in the crystal edges, range between 357±15 and 309±12Ma. They were interpreted as subsequent growths due to the peak metamorphic conditions that affected the Getic basement at 358-316Ma (Medaris *et al.,* 2003). This effect is also present on zircons from other Ordovician metagranitoids in the Sebeş-Lotru terrane which suffered Variscan partial or total resetting during an eclogite-grade metamorphic event (Balintoni and Balica, 2010).

Zircon geochemistry and significance

Zircon is one of the minerals in igneous and metamorphic rocks that host for significant fractions of the whole-rock abundance of U, Th, Hf and REE, elements used as source and process indicators or parent isotopes for age determination. Compositional investigation on zircon crystals is related to zircon role in igneous and metamorphic petrogenetic processes (Hoskin and Schaltegger, 2003; Rubatto, 2002). Based on these considerations, the trace-element geochemistry of the dated zircon zones from STG and BG samples was used to verify the accuracy of the age interpretation for each process that generated the zircon growth.

According to Grimes *et al.* (2007), zircon trace-element signature may provide information on magma sources, discriminating between crystals formed in oceanic crust from those formed in continental crust. In this regard, the BG zircon cores with ages of 677-583Ma, interpreted as belonging to the main source, have two of the U/Yb ratio of extremely low values (<0.1) that "are almost certainly derived within a MORB-type setting" whereas other two ratios have low values, typical for lower crust (Grimes *et al.,* 2015). All the inherited zircons plot in the field of ultramafic, mafic, intermediate and alkaline rocks in the Hf vs. Y diagram (Fig. 5A).

The study on trace elements of BG and STG zircons (Table II) as petrogenetic process indicators was meant to check the accuracy of the age data interpretation. The most developed oscillatory zoned areas at 493-434Ma have low U (114-396ppm) and Th (110-241ppm) contents and Th/U ratios of 0.5-1 (≥0.5) typical for igneous crystallized zircons (Hoskin and Black, 2000). Rich HREE, positive Ce and strong negative Eu anomalies (Fig. 5B) confirm the characteristics of zircons generated by igneous growth (Hoskin and Schaltegger, 2003). The outer rims of 357-309Ma have high to very high U (553-3891ppm) and Hf (9037-9952ppm) contents, extremely low Th/U (0.032-0.200) ratios, depleted HREE contents and no/small positive Ce anomalies along with no/small negative Eu anomalies (Fig. 5C), in obvious contrast with trace-element behavior in the igneous crystallized zones. These characteristics represent completely recrystallized zircons (as described by Pan, 1997 in Hoskin and Schaltegger, 2003), the flat HREE patterns and the lack of significant Eu anomalies being typical for eclogite-facies zircons (Rubatto, 2002).

DISCUSSIONS

Comparative study and petrogenetic considerations

The limited STG-BG differentiation extent, the absence of basic and intermediate related rocks in the

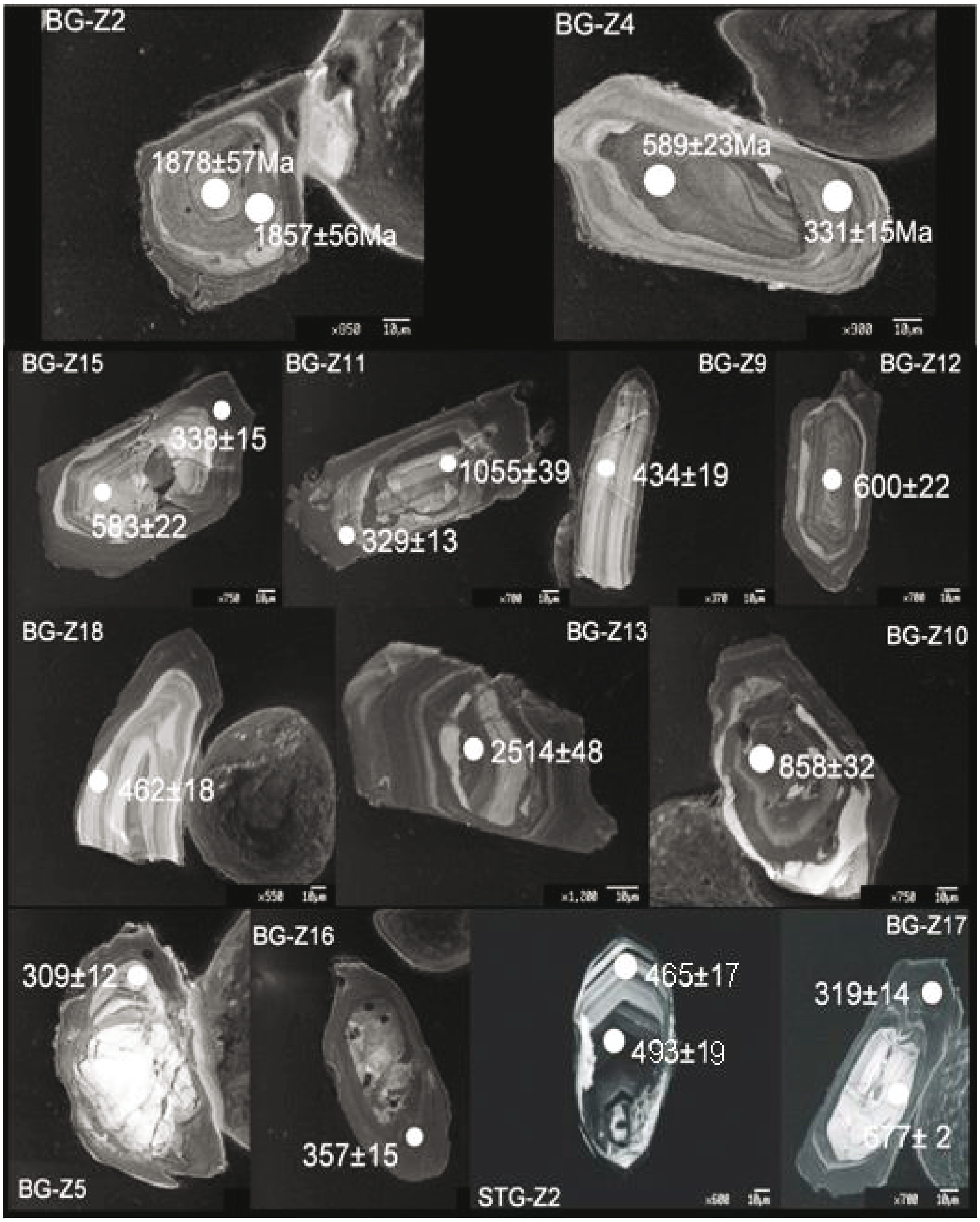

FIGURE 4. Cathodoluminescence images on the dated zircon crystals with the analyzed spots (Dobrescu *et al.*, 2010).

area and the sample plot in the La/Yb vs. La diagram (Fig. 6) indicate that partial melting was the main genetic process. Besides, the presence of inherited zircons is an argument that thorough and extensive fractionation did not occur during ascent (Miller *et al.*, 2003). Petrographically similar, the two granitoids have common I-type minerals like hornblende, green to greenish-brown biotite, epidote, zoned allanite, sphene and magnetite, contrasting with reddish-brown biotite and monazite as S-type minerals in the STG rocks. Major-element geochemistry of high Na_2O contents, A/CNK values of (0.93-1.09) with positive A/CNK-SiO_2 correlation for BG samples and negative P_2O_5-SiO_2 correlation for both granitoid samples (Fig. 2A, B) are common features for I-type granites (Chappell, 1999, Clemens and Stevens, 2012). According to Clemens and Stevens (2012) initial $^{87}Sr/^{86}Sr$ ratios of less than 0.708, between 0.704 and 0.706 (Chappell and White, 2001) for both BG and STG rocks, are typical characteristics for I-type granites derived from juvenile oceanic crust source. Variations to peraluminosity for STG samples (including slightly higher $^{87}Sr/^{86}Sr_i$ ratios) indicate an increased continental material input.

Rocks with medium-high SiO_2, high Na_2O and Al_2O_3, low Y (<18ppm), medium-high Sr contents and Sr/Y ratios, low HREE (Yb <1.8ppm) and no Eu anomaly (Fig. 3B) differ from those produced by fractional crystallization in a typical calc-alkaline arc (high HREE, low REE fractionation and negative Eu anomalies) (Peacock *et al.* 1994). Most geochemical characteristics of STG-BG rocks overlap HSA and TTG patterns (Table 2) which were interpreted as results of amphibolite/eclogite partial melting in increased pressure conditions, leaving amphibole, garnet, clinopyroxene and plagioclase residual phases (Defant and Drummond, 1990; Martin *et al.*, 2005; Rollinson and Martin, 2005). The differences from HSA (Table 2) consist in lower Mg# (18-20) values, Ni (1-5ppm) and Cr (7-16ppm) contents in STG rocks, increasing to

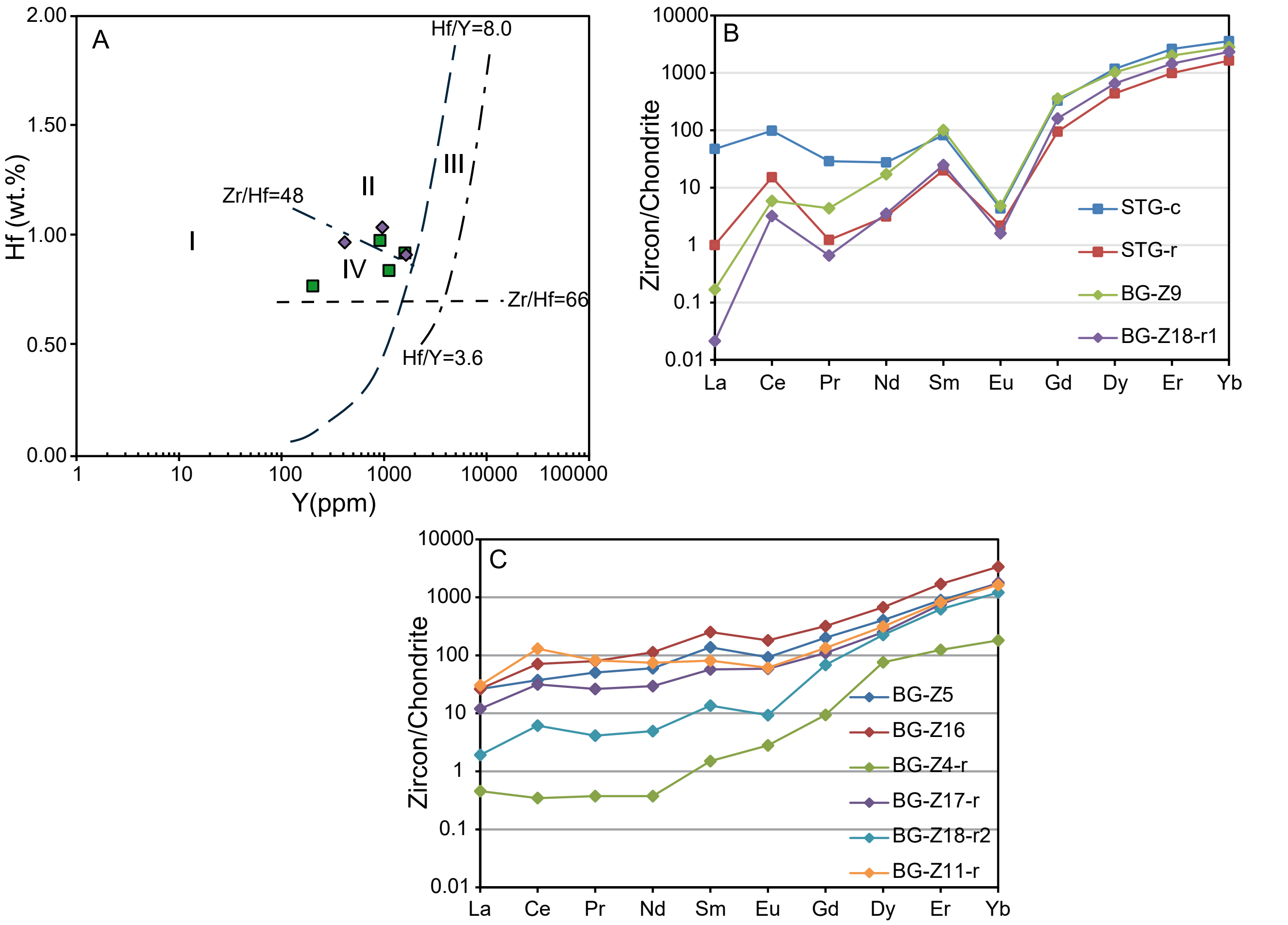

FIGURE 5. A) Hf vs. Y contents of the dated BG zircon zones relative to the fields of zircon composition defined by Shnukov *et al.* (1997) (in Belousova *et al.*, 2002): I (kimberlites); II (ultramafic, mafic and intermediate rocks); III (quartz-bearing intermediate and felsic rocks); IV (alkaline rocks)= field VI in Belousova *et al.* (2002); violet rombs (inherited zircons), green squares (main source zircons); B) chondrite-normalized REE characteristics of zircon zones interpreted as igneous crystallized; C) chondrite-normalized REE characteristics of zircon zones interpreted as recrystallized.

Mg# (29-35), Ni (6-30ppm) and Cr (19-65ppm) in BG rocks, but still lower than those of slab-derived adakitic melts enriched in interaction with mantle wedge during magma ascent (Mg#>47, average Ni contents of 20ppm and Cr of 41ppm (Smithies, 2000; Martin *et al.,* 2005). Such geochemical patterns mostly overlap Archean TTG and adakitic rocks as products of melts derived from thickened lower crust and melts resulted from experiments on wet mafic rocks (Fig. 7A, B). Similar characteristics are also present in magmas generated by slab melting during the rare cases of subduction at low angle where adakitic signature is coupled with low to slightly increasing mantle influence (Martin, 1999). Other indicators based on trace-element behavior are used in order to find out sources and P-T conditions for the STG-BG petrogenesis. As $(Sm/Yb)_N$ is a good marker of amphibole-dominated $(Sm/Yb)_N$<4 vs. garnet dominated $(Sm/Yb)_N$>5 fractionation in granitoids, its values from 2.8 to 9.4 indicate that residual assemblage is amphibole-rich, but mostly garnet-rich. Medium-high Sr contents and small/no Eu anomalies relate to minor plagioclase left in the residue. Decreasing Yb and Y while increasing Sr contents (Fig. 3A) may indicate increasing residual garnet/plagioclase ratios from STG to BG. Low HREE, $(Gd/Yb)_N$ >1 and La/Yb >20 indicate residual garnet that, together with negative Nb-Ti anomalies, relate to residual Ti-phase and low-Mg amphibole implying a garnet-bearing source-rock, probably of amphibolite type (according to Castillo (2012); Moyen (2009) criteria). The analyzed samples in diagrams like Sr/Y vs. Y (Fig. 8A), La/Yb vs. Yb (Fig. 8B) and La/Yb vs. Sr/Y (Fig. 8C) confirm the adakitic/TTG signature. The rocks plot within TTG and close to the adakite areas on Nb/Ta-Zr/Sm diagram (Fig. 8D), not far from the products of amphibolite batch melting (Foley *et al.,* 2002); taking into account Rapp *et al.* (2003) conclusions on a typical Archean basalt source, the samples are close to the eclogite melting field. Considering the low HREE and Nb, medium Ta and mid-high Sr contents, STG-BG rocks could be identified as medium-high pressure TTGs (according to Halla *et al.,* 2009 and Moyen, 2011 in Moyen and Martin, 2012) in equilibrium with residual garnet±rutile and scarce plagioclase. Despite the Nb-Ti negative anomalies indicating residual rutile, its presence as a residual phase becomes questionable because the lack of negative Ta anomalies, clinopyroxene, garnet and biotite being alternative residual phases. Considering scarce residual plagioclase consistent with low H_2O content in case of dehydrating melting at pressures up to 1.8GPa, residual garnet (stable above 1GPa) and absence of rutile (with lower stability limit at 1.5GPa (Xiong *et al.,* 2011)), the presumed melting pressure is of 1-1.5GPa. According to Moyen (2009), the Sr/Y ratios may reflect the pressure melting or inherit the source-rock Sr/Y signature. Low Mg# (18.8-20) and Sr/Y ratios (48-87) in STG rocks may relate to melting of a low-Mg# source at pressures ≥1.3 up to ~1.8GPa (Fig. 9). The composition of BG rocks seems

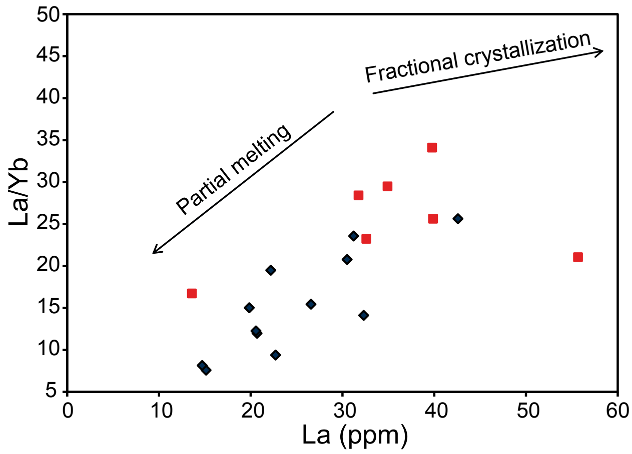

FIGURE 6. La/Yb vs. La diagram illustrating the partial melting and fractionation effects. Vectors for Fractional Crystallization (FC) and Partial Melting (PM) are from Thirwall *et al.* (1994).

to adjust to a more mafic source with higher Mg# (29.4-34.5) and Sr/Y ratios (100-175) at pressures ranging from 1.3 to 1.5GPa. A comparison with experimental results of Qian and Hermann (2013) on hydrous mafic lower crust material (Fig. 3A), based on trace-element behavior and stable mineral phases, indicates a pressure melting of ~1.25GPa and temperatures of ~900ºC. Melting in such conditions could produce negative Nb-Ti anomalies and Ta enrichment due to residual amphibole, garnet, scarce plagioclase and clinopyroxene over orthopyroxene as a main mineral residue. In STG case, because allanite is not stable at higher temperature as LREE enter the melt (Herman, 2002 in Qian and Herman, 2013), its presence together with apatite, titanite and rutile in the rock may relate to a garnet amphibolite residue left after partial melting at temperatures around 800ºC and pressure of ~1.5GPa. Lower REE contents of BG samples may indicate more residual titanite and allanite, while rutile presence at >1.25GPa and 900ºC (Qian and Hermann, 2013) could adjust to a garnet granulite. However, most granulite crustal lithologies contain abundant plagioclase which would cause Eu anomalies in any melt separated from them. Therefore, the lack of Eu anomalies in STG-BG rocks argues against granulite sources (Girardi *et al.,* 2012); instead, eclogite is a more possible source for BG magma, given the high Sr/Y and low Nb/Ta ratio significance (Rapp *et al.,* 2003).

Zircon thermometry

In an attempt to find out the temperatures attained by STG-BG magma and check the estimated partial melting thermal conditions for its genesis, as well as to explain the rich zircon inheritance in the BG rocks, both zircon saturation thermometer and Ti-in zircons thermometer have been applied.

TABLE 2. Comparison between STG, BG, HSA and TTG rocks (data from Defant and Drummond, 1990; Martin *et al.*, 2005; Moyen and Martin, 2012; Smithies, 2000). Av.= Average

Geochemical characteristics	HSA	TTG	STG	BG
SiO_2 (wt.%)	$\geq$56	$\geq$64	65.62–68.41	67.87–73.64
Al_2O_3 (wt.%)	$\geq$15 at 70% SiO_2	>15	16.59–17.19	15.21–16.11
Na_2O (wt. %)	3.5-7.5	3-7	3.86-5.17	4.62-6.40
K_2O/Na_2O	Av.= 0.47	Av.< 0.44	0.33–0.98	0.51–0.82
Sr (ppm)	>400	400-600	554-722	608–965
Y (ppm)	$\leq$18	<20	6-12	4–10
Yb (ppm)	<1.8	<1.8	0.38–1.23	0.41–0.88
Nb (ppm)	6	$\leq$10	9.1–10.4	4.3–9.5
$(La/Yb)_N$	$\geq$10	>15	22.78–39.93	10.56-30.55
Gd/Yb	3.4	3.6	1.8–6.1	3–5.1
Sr/Y	>40	>40	48-87	100–175
Mg #	Av.= 48	Av.= 38-43	18-20 Av.= 19	29.4-35 Av.= 31
Ni (ppm)	Av.= 20	Av.= 18	Av.= 2	Av.=13
Cr (ppm)	Av.= 41	Av.= 34	Av.= 11	Av.= 32

For intrusions with abundant inherited zircons, Miller *et al.* (2003) showed that zircon saturation temperature (T_{Zr}) provides useful approximation of melt-generation temperature. The calculated T_{Zr} using the expression of Watson and Harrison (1983) range within 847-897ºC for BG and 873-918ºC for STG (Table I) which contain maxima for magmas that carry zircon crystals, placing them into 'hot granites' category. Contrary to the idea that 'hot granites' have little or no inheritance (Miller *et al.*, 2003), BG rocks are rich in inherited zircons (no observation on STG sample).

In order to estimate the lower limit for the maximum temperature reached by magma and to evaluate the survival capacity of the inherited crystals, the Ti concentration of each dated zircon was used to apply the Ti-in zircons thermometer (Watson and Harrison, 2005; Watson *et al.*, 2006) on both inherited and neo-formed zircon crystals. Corrected Ti-in-zircon crystallization temperatures were calculated using the recalibrated Ti-in-zircon equation of Ferry and Watson (2007). The extremely low TiO_2/Zr ratios (0.0013-0.0031) of STG and BG rock samples indicate that melts have been severely TiO_2 undersaturated at near-liquidus conditions, fact that imply corrections of low a_{TiO2} values (0.1-0.3) applied to the Ti-in-zircon crystallization temperature formula (Schiller and Finger, 2019). Plausible crystallization temperatures were obtained using a_{TiO2} values of 0.3.

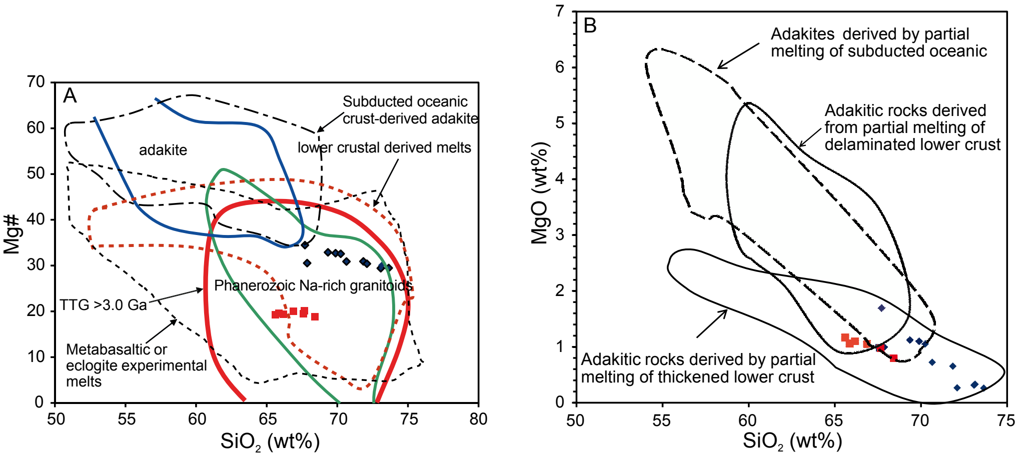

FIGURE 7. Differences from real adakites in diagrams: A) #Mg vs. SiO_2 diagram with STG-BG rocks, Archean TTG and adakite composition (TTG area from Drummond *et al.* (1996); adakite and Phanerozoic Na-rich granitoid areas from Smithies (2000); experimental liquids from Rapp *et al.*(1991), Winther (1996), Wylie *et al.* (1997) in Condie (2005); B) MgO vs. SiO_2 for the studied samples relative to adakites derived by partial melting of subducted oceanic crust, delaminated lower crust or thickened lower crust (after Wang *et al.*, 2007 and references therein).

Silica-rich rocks infer a_{SiO_2}= 1, thus requiring no correction. The calculated temperatures for zircons crystallized from STG magma range between 759ºC and 875ºC and for zircons crystallized from BG magma between 911ºC and 985ºC (Table II). As for the inherited zircons, application of Ti-in-zircon thermometer is often hindered by the lack of information regarding their host rock and by the contrasting correction values proposed for a_{TiO_2} (0.15-0.63), which would result in extremely different temperatures (Chamberlain *et al.,* 2014). However, the BG inherited zircons seem to belong mainly to oceanic crust rocks identified in ultramafic, mafic, intermediate and alkaline rocks area (Fig. 5A). Consequently, the applied correction for a_{TiO_2} is 0.7 (as proposed in Grimes *et al.,* 2009). The calculated crystallization temperatures of the oldest BG inherited zircons range between 754ºC and 921ºC and those of zircons interpreted as belonging to the main source between 681ºC and 853ºC.

The highest crystallization temperature of the BG neo-formed Ordovician zircons (within 911-985ºC interval) represents an estimate of the magma's thermal peak and an indicator of the attained partial melting thermal conditions. The crystallization temperatures obtained on STG neo-formed Ordovician zircons fully confirm the partial melting temperatures estimated by the qualitative modelling on whole-rock geochemistry.

Usually, pre-magmatic zircons survive when magma temperature is not high enough to dissolve them or when kinetic effects hinder their dissolution (Bea *et al.,* 2007). The temperatures calculated using Ti-in-zircon thermometer on neo-formed Ordovician zircon crystals of BG rocks reached and even exceeded 900ºC. It seems that survival of old zircons was possible in this case despite the temperatures reached by magma, high enough (exceeding the BG rocks T_{Zr} values of 847-897ºC) to dissolve almost all the inherited zircons. Under equilibrium conditions, the temperature for total zircon dissolution in a magma roughly corresponds to T_{Zr} which does not surpass 870ºC (Bea *et al.,* 2007). Among the dated zircons, there is only one exception of BG zircon core with crystallization temperature higher than the peak magma temperature, crystal that would have survived anyway. The rest of the old zircon cores survived because of other reasons. According to Bea *et al.,* (2007) referring to the Central Iberian Cambro-Ordovician igneous rocks with similar unusual situation, the explanation for the zircon survival when magma temperature exceeds their crystallization temperature is related either to kinetic effects that hinder their dissolution or to incomplete dissolution that could occur due to the short life-span of magmatic pulses.

TECTONIC SETTING

The geochemistry of STG-BG rocks characterized by adakitic signature was interpreted to originate mainly from partial melting of garnet-bearing rocks of amphibolite, eclogite and less probable of granulite type. The few peraluminous features and the rich zircon inheritance indicate addition of old continental crust/sediments to the source; on the other hand, low to increasing mantle influence affected the magmas. Usually, garnet amphibolite/eclogite/granulite rocks occur at 30-40km depth in the crust where partial melting could have triggered. According to Girardi *et al.* (2012), magmas of lower $(La/Yb)_N$ ratios with no Eu anomalies (as observed in STG-BG rocks) have deeper sources than 40km.

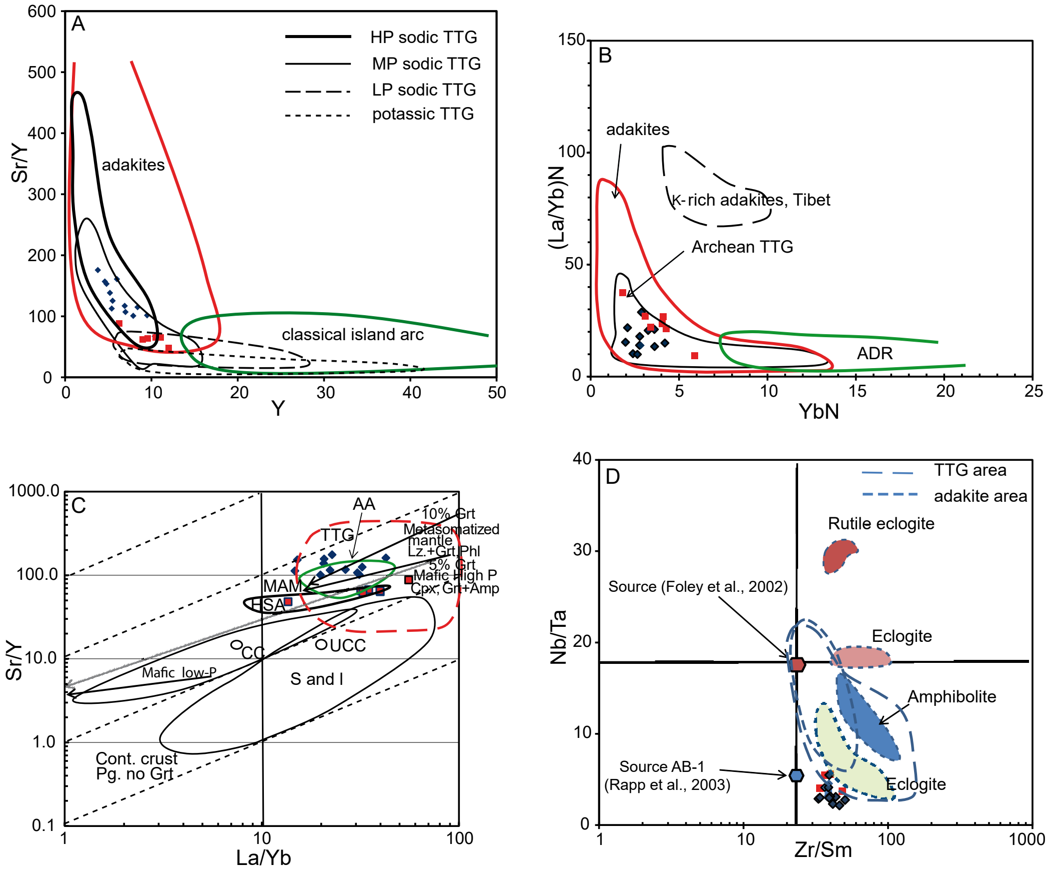

FIGURE 8. Comparison between STG-BG rocks, HSA and TTG in diagrams: A) Sr/Y vs. Y diagram (Defant and Drummond, 1990; Martin, 1999). HP (high-pressure) sodic TTG, MP (medium-pressure) sodic TTG, LP (low-pressure) sodic TTG and potassic TTG areas from Moyen (2011); B) La/Yb)N vs.YbN diagram discriminating between adakites, K-rich adakites (Wang *et al.*, 2005), Archean TTG and classical island arc calc-alkaline suites; C) Sr/Y vs. La/Yb diagram (Moyen, 2009) representing models of melting and mantle interactions: black line area (HSA), red dashed line area (TTG), green line area: Archean Adakites (AA), black line area: normal granites "S and I"; CC (Continental Crust), UCC (Upper Continental Crust), MAM (Mantle Adakite Mix); Mafic low-P (1.0GPa) melting with a garnet-plagioclase residuum; Mafic high-P (2.0GPa) melting of a similar source generating HSA-like melts; D) Nb/Ta vs. Zr/Sm diagram for STG-BG samples compared with TTG and adakites and the possible modeled sources for TTG. The different sources are represented by red and blue fields from Foley *et al.* (2002) and green field from Rapp *et al.* (2003) discussed in Moyen and Martin (2012); the TTG and adakite areas are from Richards and Kerrich (2007).

The analyzed samples on a tectonic discrimination diagram (Fig. 10) indicate magmas related to a volcanic arc setting; the rocks are LILE-enriched and HFSE-depleted (Nb-Ti negative anomalies), typical for subduction-related magmas. Granitoids with adakitic signature formed in a subduction setting are linked to slab melting within extremely limited conditions such as high geothermal gradient, relatively hot and young oceanic crust or fast/flat subduction and slab window, where dehydration melting of hydrated minerals occurs (Defant and Drummond, 1990; Gutscher *et al.*, 2000; Yogodzinski *et al.*, 2001). The peraluminous characteristics observed in STG rocks coupled with low #Mg and heavy metals contents may be interpreted as sedimentary input from the subducted plate and low mantle influence on a prime magmatic pulse, followed by a metaluminous melt affected by increased mantle influence, as a second BG magmatic pulse. These geochemical features may restrict the tectonic setting to slab melting during a subduction at low angle. The sequence of magmatic pulses revealed by the intrusion age intervals at 493-465Ma for STG followed by 462-434Ma for BG and the trace-element behavior with frequent parallel trends support the hypothesis. The calculated depth of melting (d_m) at crustal/mantle limit in subduction-related arcs based on $(La/Yb)_N$ ratios, on samples within 65-68wt.% SiO_2 range (protocol applied from Chapman *et al.*, 2015 in Profeta *et al.*, 2015) with [d_m= 21.277 ln (1.0204 $(La/Yb)_N$] formula, averages 69km for STG and 70km for BG. According to Balintoni *et al.* (2010), a tectonic extension took place since late Cambrian until ~470Ma followed by contraction between 470 and 450Ma, when a double subduction was presumed, continental arc granites emplacement being accompanied by metamorphism and deformation.

The occurrence of the STG-BG strata-like intrusions at the same level with eclogitic bodies in the LMS connects

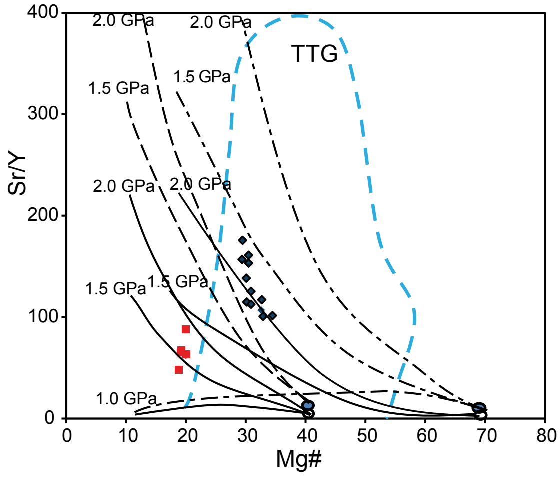

FIGURE 9. Samples of STG-BG on Mg# vs. Sr/Y diagram: melting models of MORB-type source (Mg#= 70) and felsic crustal source (Mg#= 40), each with low Sr/Y (=3) source (solid curves) and higher Sr/Y (=10) source (dashed curves) (Moyen, 2009).

their history to the subduction-collisional geotectonic model of the emplacement of eclogites advanced by Săbău and Massone (2003). Related to this image, STG-BG could have formed by partial melting of garnet-bearing rocks in a tectonic mélange at the continental crust/oceanic crust/mantle contact, where rocks with diverse thermo-baric evolution were put together during collision that occurred in front of a subduction zone, during Caledonian orogeny. The actual Getic basement contains strongly deformed metasediments, eclogites, ultramafic and mafic rocks, suggesting an accretion complex composed of oceanic and continental components (Conovici, 2000; Săbău and Massone, 2003). The lowest level basement lithology in the Semenic Mountains exhibits basic rocks and garnet-granulites (Conovici, 2000) which may belong to garnet-bearing residues left after generating melts of STG-BG type. The presumed P-T conditions for adakites/TTG genesis are close to the peak metamorphic conditions for some granulites which may represent residues of adakite/TTG magmas (Jiang *et al.*, 2007; Nehring *et al.*, 2009, 2010; Storkey *et al.*, 2005 in Qian and Hermann, 2013). A more plausible scenario for the STG-BG magma genesis could be related to exhumation of high-pressure metamorphic rocks from the lower-crust (where these were tectonically first emplaced) into the upper crust. In order to quantify the crustal thickness/Moho depth (D_M) and to find out the depth at which partial melting could have triggered, D_M= 27.78 ln[0.34$(La/Yb)_N$] formula was applied (Hu *et al.*, 2017). The results indicate ~60km calculated on STG samples and ~50km on BG samples. According to Săbău and Massone (2003) eclogites that occur in LMS, originating from both subducted oceanic crust and mantle cumulates, were emplaced in the upper crust by a succession of syn-subduction exhumation of detached slab fragments. During this process, garnet-amphibolites and eclogites could have been partially melted by decompression and heating at crustal depth of 60-50km, at P-T conditions of around 1.5GPa and 900-800ºC. The spatial disposal of eclogites and granitoids suggests that both types were enclosed in the buoyant mélange from the subductive margins during the subduction-collision process and placed randomly between the two continental blocks (SN and VU).

CONCLUSIONS

The study on the STG-BG rocks identified granitoids with predominantly I-type and few S-type features, but also geochemical characteristics that approximate the adakitic signature. Qualitative modeling and whole-rock geochemistry provide benchmarks on residues and sources of garnet-bearing rocks of amphibolite and eclogite type, partially melted at pressures exceeding 1.25GPa and temperatures of 800-900ºC (confirmed by calculated Ti-in zircon temperatures). Particularities related to low to slightly increasing heavy metals contents and $^{87}Sr/^{86}Sr$ ratios along with rich zircon inheritance argue for an oceanic crust source affected by minor to increasing mantle influence, enriched with old crustal material. The geochemical differences between the two granitoids indicate that they could have formed from two distinct magmatic pulses generated by slab melting during a subduction process, under particular low angle conditions. An alternative model for the STG-BG genesis could relate to partial melting of garnet-amphibolites and eclogites due to decompression and heating at crustal depth (60-50km) and P-T conditions of around 1.5GPa and 900-800ºC, during syn-subduction exhumation of eclogitized slab fragments. The granitoids

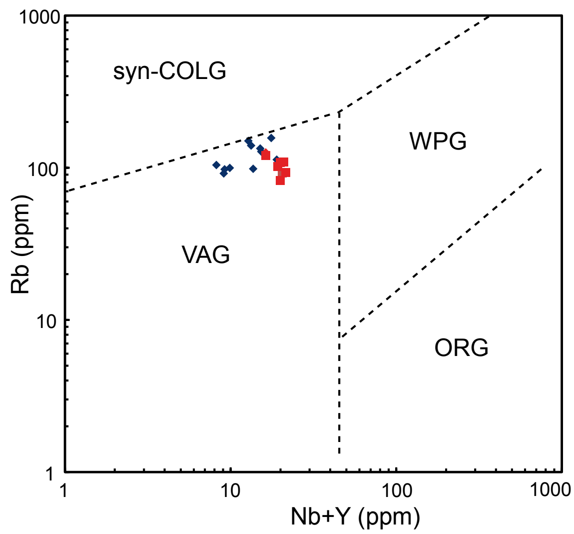

FIGURE 10. Trace-element geotectonic diagram of Pearce *et al.* (1984) for STG-BG.

must have been entrained into a buoyant mélange from the subductive margins during the collision and placed randomly between two continental units.

U-Pb zircon ages obtained on the newly formed crystals, interpreted as Ordovician igneous crystallization time and Variscan recrystallization imprints, were confirmed by the trace elements characteristics of the dated zircon zones, thus relating the STG-BG magmatism to a pre-Variscan subduction-collision event. The rich zircon inheritance reveals Neoproterozoic contribution to the source and recycling of older crustal components of Neoarchean to Paleoproterozoic ages.

ACKNOWLEDGMENTS

Rock analyses were financed by EU Large Scale Geochemical Facility Program (2003) and performed at Bristol University under the assistance of Chung Choi. Dorin Dordea helped in field and laboratory work and Julieta Rusu in sample preparation at Prospecțiuni SA. U/Pb dating was financed by the Romanian Ministry of Education and Research (CEEX-M1-C2-4230/2006-2008 project) and performed at CNR-Istituto di Geoscienze e Georisorse, Unita di Pavia thanks to Massimo Tiepolo and Elena Negulescu. I am grateful to Mihai Conovici, Haralambie Savu, Mihai Tatu and Peter Luffi for valuable talks and corrections. SIMS analyses were financed by UEFISCDI grant PN-III-P1-1.1-MC-2017-2295 and performed by Martin Whitehouse and Gavin Kenny at NORDSIM, Stockholm. Loving hugs to my Canadian family for correcting English. The author is grateful to reviewers and editors for constructive comments and suggestions that improved the manuscript.

REFERENCES

Atherton, M.P., Petford, N., 1993. Generation of sodium-rich magmas from newly underplated basaltic crust. Nature, 362, 144-146.

Balica, C., 2007. Age and origin of the metamorphic units of the South Carpathians and Apuseni Mountains with possible implications on the Pre-Alpine termotectonic evolution (in Romanian). PhD Thesis. Cluj-Napoca, University of Cluj, 212pp.

Balintoni, I., 1997. Geotectonics of Romanian Metamorphic Terrains (in Romanian). Cluj-Napoca, Editura Carpatica, 176pp.

Balintoni, I., Balica, C., Ducea, M.N., Fukun, C., Hann, H.P., Sabliovschi, V., 2009. Late Cambrian-Early Ordovician Gondwanan terranes in the Romanian Carpathians A zircon U-Pb provenance study. Gondwana Research, 16, 119-133.

Balintoni, I., Balica, C., 2010. The high U zircons, recorders of the post-crystallization thermotectonic events. Goldschmidt Conference Abstracts, A44.

Balintoni, I., Balica, C., Ducea, M.N., Hann, H.P., Sabliovschi, V., 2010. The anatomy of a Gondwanan terrane. The Neoproterozoic-Ordovician basement of the pre-Alpine Sebeş-Lotru composite terrane (South Carpathians, Romania). Gondwana Research, 17, 561-572.

Balintoni, I., Balica, C., Ducea, M.N., Hann H.P., 2014. Peri-Gondwanan terranes in the Romanian Carpathians A review of the spatial distribution, origin, provenance, and evolution. Geosciences Frontiers, 5(3), 395-411.

Bayanova, T., Ludden, J., Mitrofanov, F., 2009. Timing and duration of Palaeoproterozoic events producing ore-bearing layered intrusions of the Baltic Shield: Metallogenic, petrological and geodynamic implications. Geological Society London Special Publications, 323(1), 165-198. DOI: 10.1144/SP323.8

Bea, F., Montero, P., Gonzalez-Lodeiro, F., Talavera, F., 2007. Zircon Inheritance Reveals Exceptionally Fast Crustal Magma Generation Processes in Central Iberia during the Cambro-Ordovician. Journal of Petrology, 48, 2327-2339. DOI: 10.1093/petrology/egm061

Belousova, E.A., Griffin, W.L., O'Reilly, S.Y., Fisher, N.J., 2002. Igneous zircon: Trace element composition as an indicator of source rock type. Contributions to Mineralogy and Petrology, 143, 602-622. DOI: 10.1007/s00410–002–0364–7

Castillo, P.R., 2006. An overview of adakite petrogenesis. Chinese Science Bulletin, 51, 257-268.

Castillo, P.R., 2012. Adakite Petrogenesis. Lithos, 134, 304-316.

Chamberlain, K.J., Wilson, C.J.N., Wooden, J.L., Cherlier, B.L.A., Ireland, T.R., 2014. New perspectives on the Bishop Tuff from zircon textures, ages and trace elements. Journal of Petrology, 55, 395-426. DOI: 10.1093/ petrology/egt072

Chappel, B.W., 1999. Aluminium saturation in I- and S-type granites and the characterization of fractionated haplogranites. Lithos, 46, 535-551.

Chappell, B.W., White, A.J.R., 2001. Two contrasting granite types: 25 years later. Australian Journal of Earth Sciences, 48, 489-499.

Clemens, J.D., Stevens, G., 2012. What controls chemical variations in granitic magmas? Lithos, 134-135, 317-329.

Condie, K.C., 2005. TTGs and adakites: are they both slab melts? Lithos, 80(1-4), 33-44.

Conovici, M., 2000. Geostructural study on the Getic-Supragetic domain from the south-western part of the South Carpathians (in Romanian). PhD Thesis. Cluj-Napoca, Babeş-Bolyai University, 224pp.

Defant, M.J., Drummond, M.S., 1990. Derivation of some modern arc magmas by melting of the subducted lithosphere. Nature, 347, 662-665.

Dimitrescu, R., 2007. The Neresnica-Poniasca granitoids and their prolongations within the South Carpathians. Proceedings of the Romanian Academy, 9-1, 33-35.

Dobrescu, A., Tiepolo, M., Negulescu, E., Dordea, D., 2010. U/Pb zircon geochronology on TTG rocks from South Carpathians (Romania) insights into the geologic history of the Getic crystalline basement. Greece, Proceedings of the XIX CBGA Congress, Scientific Annals of the School of Geology,

Aristotle University of Thessaloniki, 99 (Special volume), 225-232.
Drummond, M.S., Defant, M.J., 1990. A model for trondhjemite-tonalite-dacite genesis and crustal growth via slab melting Archaean to modern comparisons. Journal of Geophysical Research, 95, 21503-21521.
Drummond, M.S., Defant, M.J., Kepezhinskas, P.K., 1996. The petrogenesis of slab-derived trondhjemite-tonalite-dacite/adakite magmas. Transactions of the Royal Society of Edinburgh Earth Sciences, 87, 205-215.
Duchesne, J-C., Liegeois, J-P., Iancu, V., Berza, T., Matukov, D.I, Tatu, M., Sergeev, S.A., 2008. Post-collisional melting of crustal sources constraints from geochronology, petrology and Sr, Nd isotope geochemistry of the Variscan Sichevita and Poniasca granitoid plutons (South Carpathians, Romania). International Journal of Earth Sciences, 97, 705-723.
Ferry, J.M., Watson, E.B., 2007. New thermodynamic models and revised calibrations for the Ti-in-zircon and Zr-in-rutile thermometers. Contribution to Mineralogy and Petrology, 154, 429-437.
Foley, S., Tiepolo, M., Vannucci, R., 2002. Growth of early continental crust controlled by melting of amphibolite in subduction zones. Nature, 417, 637-640.
Girardi, J.D., Patchett, P.J., Ducea, M.N., Gehrels, G.E., Robinsoncecil, M., Rusmore, M.E., Woodsworth, G.J., Pearson, D.M., Manthei, C., Wetmore, P., 2012. Elemental and isotopic evidence for granitoid Genesis from deep-seated sources in the Coast Mountains Batholith, British Columbia. Journal of Petrology, 53, 1505-1536.
Gridan, T., 1981. The petrology of the north-eastern part of the Semenic Mountains (in Romanian). Bucureşti, Editura Academiei Romane, 194pp.
Grimes, C.B., John, B.E., Kelemen, P.B., Mazdab, F., Wooden, J.L., Cheadle, M.J., Hanghøj, K., Schwartz, J.J., 2007. The trace element chemistry of zircons from oceanic crust a method for distinguishing detrital zircon provenance. Geology, 35, 643-646. DOI: 101130/G23603A1
Grimes, C.B., John, B.E., Cheadle, M.J., Mazdab, F.K., Wooden, J.L., Swapp, S., Schwartz, J.J., 2009. On the occurrence, trace element geochemistry, and crystallization history of zircon from in situ ocean lithosphere. Contribution to Mineralogy and Petrology, 158, 757-783. DOI: 10.1007/s00410-009-0409-2
Grimes, C.B., Wooden, J.L., Cheadle, M.J., John, B.E., 2015. "Fingerptinting" tectono-magmatic provenance using trace elements in igneous zircon. Contribution to Mineralogy Petrology, 170:46, 1-26. DOI: 10. 1007/s00410-015-1199-3
Gutscher, M-A., Maury, R., Eissen, J-P., 2000. Can slab melting be caused by flat subduction? Geology, 28, 535-538.
Henderson, P., 1984. Rare Earth Element Geochemistry. Amsterdam, Elsevier, 510pp.
Hickey-Vargas, R., Moreno Roa, H., Lopez Escobar, L., Frey, F.A., 1989. Geochemical variations in Andean basaltic and silicic lavas from the Villarica-Lanin volcanic chain (395ºS) an evaluation of source heterogeneity, fractional crystallisation and crustal assimilation. Contribution to Mineralogy and Petrology, 103, 361-386.
Hoskin, P.W.O., Black, L.P., 2000. Metamorphic zircon formation by solid-state recrystallization of protolith igneous zircon. Journal of Metamorphic Geology, 18, 423-439.
Hoskin, P.W.O., Schaltegger, U., 2003. The Composition of Zircon and Igneous and metamorphic Petrogenesis. Reviews in Mineralogy and Geochemistry, 53(1), 27-62.
Hu, F., Ducea, M.N., Liu, S., Chapman, J.B., 2017. Quantifying Crustal Thickness in Continental Collisional Belts: Global Perspective and a Geologic Application. Scientific Reports, 7:7058, 1-10. DOI: 10.1038/s41598-017-07849-7
Iancu, V., Mărunăiu, M., 1989. Toroniţa Zone and problems of the pre-Alpine metamorphic basement of the Getic and Danubian realms. Bucureşti, Dări de Seamă ale Institutului de Geologie şi Geofizică, 74(1), 223-237.
Iancu, V., Berza, T., Seghedi, A., Mărunţiu, M., 2005. Paleozoic rock assemblages incorporated in the South Carpathian Alpine thrust belt (Romania and Serbia) a review. Geologica Belgica, 8, 48-68.
Iancu, V., Seghedi, A., 2018. The South Carpathians: Tectono-Metamorphic Units related o Variscan and Pan-African inheritance. Geo-Eco-Marina, 23, 245-262.
Martin, H., 1999. Adakitic magmas modern analogues of Archaean granitoids. Lithos, 46, 411-429.
Martin, H., Smithies, R.H., Rapp, R.P., Moyen, J-F., Champion, D.C., 2005. An overview of adakite, tonalite-trondhjemite-granodiorite (TTG) and sanukitoid relationships and some implications for crustal evolution. Lithos, 79, 1-24.
Medaris, G., Ducea, M., Ghent, E., Iancu, V., 2003. Conditions and timing of high-pressure Variscan metamorphism in the South Carpathians, Romania. Lithos, 70, 141-161.
Miller, C., McDowell, S.M., Mapes, R.W., 2003. Hot or cold granites? Implications of zircon saturation temperatures and preservation of inheritance. Geology, 31(6), 529-532. DOI: 10.1130/0091-7613(2003)031<0529:HACGIO>2.0.CO;2
Moyen, J-F., 2009. High Sr/Y and La/Yb ratios The meaning of the "adakitic signature". Lithos, 112, 556-574.
Moyen, J-F., 2011. The composite Archean grey gneisses. Petrological significance and evidence for a non-unique tectonic setting for Archean crustal growth. Lithos, 123, 21-36.
Moyen, J-F., Martin, H., 2012. Forty years of TTG research. Lithos, 148, 312-336.
Qian, Q., Hermann, J., 2013. Partial melting of lower crust at 10-15 kbar constraints on adakite and TTG formation. Contributions to Mineralogy and Petrology, 165(6), 1195-1224.
Peacock, S.M., Rushmer, T., Thompson, A.B., 1994. Partial melting of subducting oceanic crust. Earth and Planetary Science Letters, 121, 227-244.
Pearce, J.A., Harris, N.B.W., Tindle, A.G., 1984. Trace element discrimination diagrams for the tectonic interpretation of granitic rocks. Journal of Petrology, 25, 956-983.
Profeta, L., Ducea, M.N., Chapman, J.B., Paterson, S.R., Gonzales, S.M., Kirsh, M., Petrescu, L., DeCelles, P.G., 2015. Quantifying

crustal thickness over time in magmatic arcs. Scientific Reports, 5(17786), 1-7. DOI: 10.1038/srep17786
Rapp, R.P., Watson, E.B., Miller, C.F., 1991. Partial melting of amphibolite/eclogite and the origin of Archean trondhjemites and tonalites. Precambrian Research, 51(1-4), 1-25. DOI: https://doi.org/10.1016/0301-9268(91)90092-O
Rapp, R.P., Watson, E.B., 1995. Dehydration melting of metabasalts at 8-32 kbar implications for continental growth and crustal-mantle recycling. Journal of Petrology, 36, 891-931.
Rapp, R.P., Shimizu, N., Norman, M.D., 2003. Growth of early continental crust by partial melting of eclogite. Nature, 425, 605-609.
Richards, J., Kerrich, R., 2007. Special paper Adakite-like rocks their diverse origins and questionable role in metallogenesis. Economic Geology, 102, 1-40.
Rollinson, H., Martin, H., 2005. Geodynamic controls on adakite, TTG and sanukitoid genesis implications for models of crust formation, introduction to the special issue. Lithos, 79, IX-XII.
Rubatto, D., 2002. Zircon trace element geochemistry partitioning with garnet and the link between U-Pb ages and metamorphism. Chemical Geology, 184, 123-138.
Rudnick, R.L., Gao, S., 2003. Composition of the continental crust. In: Rudnick, R.L., Holland, H.D., Turekian, K. (eds.). Treatise on geochemistry, The Crust. Elsevier, 3, 1-64.
Savu, H., 1997. On some granitods with trondhjemitic affinities from the NE Semenic Mountains - Southern Carpathians. Analele Universităţii Bucureşti, Geologie, XLVI, 41-52.
Săbău, G., 1999. Baric types of metamorphism in the Getic Crystalline significance and implications on the interpretation of the lithostratigraphic sequence (in Romanian). PhD Thesis. Bucharest, University of Bucharest, 270pp.
Săbău, G., Massone, H.J., 2003. Relationships among eclogite bodies and host rocks in the Lotru metamorphic suite (South Carpathians, Romania); petrological evidence for multistage tectonic emplacement of eclogites in a medium-pressure terrain. International Geology Review, 45, 225-262.
Săbău, G., Negulescu, E., 2012. U-Th-Pb Monazite Geochronology in the South Carpathian Basement Variscan Syn-Metamorphic Tectonic Stacking and Long-lasting Post-Peak Decompressional Overprints. AGU Fall Meeting, Control ID 1485915.
Săndulescu, M., Krautner, H.P., Borcoş, M., Năstăseanu, S., Patrulius, D., Ştefănescu, M., Ghenea, C., Lupu, M., Savu, H., Bercia, I., Marinescu, F., 1978. Geological map of Romania, scale 11,000,000. Geological Institute of Romania.
Săndulescu, M., 1984. Geotectonics of Romania (in Romanian). București, Editura Tehnica, 336pp.
Schiller, F., Finger, F., 2019. Application of Ti-in-zircon thermometry to granite studies: Problems and possible solutions. Contribution to Mineralogy and Petrology. 174 (51), 1-16. DOI: https://doi.org/10.1007/s00410-019-1585-3
Smithies, R.H., 2000. The Archean tonalite-trondhjemite-granodiorite (TTG) series is not an analogue of Cenozoic adakite. Earth and Planetary Sciences Letters, 182(1), 115-125.
Stoica, A.M., Ducea, M.N., Roban, R.D., Jianu, D., 2016. Origin and evolution of the South Carpathians basement (Romania) a zircon and monazite geochronologic study of its Alpine sedimentary cover. International Geology Review, 58(4), 510-524. DOI: https://doi.org/10.1080/00206814.2015.1092097
Sun, S.S., McDonough, W.F., 1989. Chemical and isotopic systematics of oceanic basalts implications or mantle composition and processes. Geological Society Special Publications, 42, 313-345.
Tiepolo, M., 2003. In situ Pb geochronology of zircon with laser ablation-inductively coupled plasma-sector field mass spectrometry. Chemical Geology, 192, 1-19.
Thirwall, M.F., Smith, T.E., Graham, A.M., Theodorou, N., Hollings, P., Davidson, J.P., Arculus, R.J., 1994. High field strength element anomalies in arc lavas source or process? Journal of Petrology, 35, 819-838.
Vavra, G., 1990. On the kinematics of zircon growth and its petrogenetic significance: a cathodoluminescence study. Contributions to Mineralogy and Petrology, 106(1), 90-99.
Wang, Q., Wyman, D.A., Xu, J.F., Jian, P., Zhao, Z.H., Li, C.H., Xu, W., 2007. Early Cretaceous adakitic granites in the Northern Dabie Complex, central China: implications for partial melting and delamination of thickened lower crust. Geochimica et Cosmochimica Acta, 71, 2609-2636.
Watson, E.B., Harrison, T.M., 1983. Zircon saturation revisited: temperature and composition effects in a variety of crustal magma types. Earth and Planetary Science Letters, 64, 295-304.
Watson, E.B., Harrison, T.M., 2005. Zircon thermometer reveals minimum melting conditions on earliest Earth. Science, 308, 841-844.
Watson, E.B., Wark, D., Thomas, J., 2006. Crystallization thermometers for zircon and rutile. Contributions to Mineralogy and Petrology, 151, 413-433.
Winther, T.K., 1996. An experimentally based model for the origin of tonalitic and trondhjemitic melts. Chemical Geology, 127, 43-59.
Whitehouse, M.J., Kamber, B., Moorbath, S., 1999. Age significance of U-Th-Pb zircon data from early Archaean rocks of west Greenland - a reassessment based on combined ion-microprobe and imaging studies. Chemical Geology, 160, 201-224.
Whitehouse, M.J., Kamber, B.S., 2005. Assigning dates to thin gneissic veins in high-grade metamorphic terranes a cautionary tale from Akilia, southwest Greenland. Journal of Petrology, 46(2), 291-318. DOI: 101093/petrology/egh075
Xiong, X.L., Liu, X.C., Zhu, Z.M., Li, Y., Xiao, W.S., Song, M.S., Zhang, S., Wu, J.H., 2011. Adakitic rocks and destruction of the North China Craton Evidence from experimental

petrology and geochemistry. China Earth Sciences, 54, 858-870.

Yogodzinski, G.M., Lees, J.M., Churikova, T.G., 2001. Geochemical evidence for the melting of subducting oceanic lithosphere at plate edges. Nature, 409, 500-504.

Manuscript received February 2020;
revision accepted March 2021;
published Online April 2021.

APPENDIX I

TABLE I. Major oxide and trace element analyses of STG and BG bulk samples; major elements (wt.%), trace elements (ppm); Mg#=mol.100*MgO/(MgO+FeOtot), A/CNK=mol. [Al_2O_3/(CaO+Na_2O+K_2O)], (Eu/Eu*=EuN/[(SmN+GdN)*1/2]. TZr(K)= 12900/[2.95+0.85*M+ln(496000/Zrmelt)], M=(Na+K+2Ca)/(Al*Si)

Sample	STG-19	STG-18	STG-13	STG-17	STG-14	SGT-16	BG-4	BG-1	STG-15	BG-2	BG-12	BG-11	BG-6	BG-7	BG-5	BG-9	BG-10	BG-8
Rock	*To.*	*To.*	*To.*	*Grd.*	*To.*	*To.*	*Grd.*	*To.*	*Grd.*	*Tdhj.*	*Grd.*	*Grd.*	*Tdhj.*	*Gr.*	*Tdhj.*	*Gr.*	*Gr.*	*Gr.*
SiO_2	65.62	65.88	66.19	66.88	67.59	67.66	67.7	67.87	68.41	69.34	69.88	70.24	70.65	71.85	72.10	73.08	73.14	73.64
TiO_2	0.54	0.47	0.49	0.45	0.47	0.43	0.46	0.34	0.36	0.34	0.33	0.32	0.23	0.21	0.13	0.14	0.15	0.13
Al_2O_3	17.19	16.59	16.81	16.65	17.00	16.63	16.07	16.11	16.60	15.79	15.58	15.57	15.48	15.36	15.39	15.35	15.34	15.21
Fe_2O_3	4.25	3.77	3.98	3.62	3.51	3.32	2.79	1.96	2.97	1.99	1.96	1.88	1.40	1.26	0.52	0.65	0.66	0.54
MnO	0.06	0.07	0.06	0.05	0.03	0.06	0.04	0.02	0.08	0.03	0.03	0.03	0.02	0.02	<0.01	0.01	0.01	<0.01
Mg0	1.17	1.07	1.11	1.05	0.99	0.97	1.70	1.00	0.80	1.13	1.11	1.05	0.72	0.65	0.27	0.32	0.33	0.26
CaO	3.38	3.41	3.50	2.61	3.38	3.03	2.32	2.08	2.94	1.86	1.85	1.72	1.47	1.45	1.51	1.44	1.43	1.14
Na_2O	4.39	5.17	4.11	3.86	4.52	4.16	4.78	6.40	3.97	5.03	4.62	4.68	5.59	4.72	6.27	4.91	4.89	4.94
K_2O	1.82	2.98	2.58	3.80	1.48	2.85	3.39	3.38	3.06	3.76	3.74	3.81	3.91	3.89	3.17	3.38	3.31	3.39
P_2O_5	0.21	0.18	0.19	0.16	0.19	0.17	0.17	0.16	0.13	0.14	0.13	0.12	0.11	0.09	0.06	0.05	0.06	0.06
LOI	1.11	0.37	0.89	0.73	0.84	0.66	0.56	0.64	0.61	0.59	0.57	0.60	0.44	0.54	0.62	0.71	0.71	0.72
Total	99.72	99.94	99.92	99.87	100.00	99.93	99.99	99.94	99.91	99.98	99.78	100.02	100.02	100.03	100.02	100.03	100.03	100.02
Na_2O/K_2O	2.41	1.73	1.59	1.02	3.07	1.46	1.41	1.89	1.30	1.34	1.23	1.23	1.43	1.21	1.98	1.45	1.48	1.46
#Mg	19.2	19.6	19.3	20.1	19.5	20.2	34.5	30.5	18.8	32.9	32.7	32.6	30.9	30.9	30.4	29.4	30.1	29.5
A/CNK	1.25	0.99	1.14	1.11	1.27	1.14	1.05	0.94	1.15	1.02	1.04	1.04	0.97	1.04	0.97	1.08	1.09	1.10
Rb	93	108	92	120	82	102	113	98	109	126	128	134	140	150	92	98	100	104
Sr	722	610	698	554	682	561	965	966	572	796	808	749	690	608	735	722	719	667
Ba	950	1170	1230	1790	660	1300	1010	970	1470	870	850	780	700	620	630	660	660	660
Cs	1.9	5.5	2.3	8.2	4.5	6.5	7.6	4.2	5.9	10.6	13.1	12.2	9.2	10	5.2	4.9	7.6	5.1
Zr	193	152	179	155	162	144	153	149	126	133	129	130	114	99	98	97	103	103
Hf	4.8	3.4	4.8	4.1	4.7	4	4.2	4.4	3.6	4.4	3.9	3.7	3.7	3.5	3.9	3.6	3.7	2.5
Th	15.2	11.7	14	9.2	12.4	11.2	10.6	11.6	8.9	10.4	9.4	10	8.9	8.1	12.8	12.9	11.8	11
Pb	29.3	45	35.6	48.4	34.1	42.2	59.5	66.8	52.4	65.3	66.6	70.1	81.4	81.2	65.9	65	65.5	57.5
Zn	62.4	66.3	67.4	70.8	46	60.8	64.9	57.5	67.8	52.5	52.4	51.2	43.5	40.5	14.4	17.8	17.8	12.8
Ta	1.9	1.9	3.4	2.7	1.7	2.5	3.3	1.9	< 2.0	2.4	< 2.0	2.7	1.9	2.4	2	< 1.5	1.5	< 1.6
Nb	10.4	10.4	10.1	10	9.5	10.3	9.5	7.7	9.1	8.4	8.4	8.1	7.8	7.4	4.3	4.6	4.7	4.4
Y	11.1	9.6	10.4	6.3	10.5	9	9.5	6	11.9	7.9	6.9	7	5.5	5.4	4.8	4.6	5.2	3.8
U	2.9	1.7	3.8	1.7	2.5	2.4	3.3	2.4	2.7	< 0.5	2.2	1.1	3.1	2.9	2.8	4	2.4	2.4
Ni	2.3	2	1.1	<1	4.5	1.6	29.8	8.9	0.8	17.6	16.7	15.5	11.5	10.3	5.7	8.5	7.4	6.1
Co	11.5	13	9.2	11	10.9	9.5	7.4	11.8	12.7	6.8	6.2	6.5	8.7	5.5	3.1	4.2	3.6	<2
V	35.2	36	36.1	39.7	35.6	36.1	53	33.7	21	39.7	38.6	33.3	15.1	16.2	11	12.8	11.7	11.2
Cr	16.2	11.6	8.7	11.6	12.2	12.6	64.8	20.9	6.9	34.6	36.7	34.2	53.7	23.7	21.8	21	18.9	18.6
Ga	20	20.1	19.5	18	20	19.5	22.3	21.2	19.1	21.4	22.7	23	23	23.1	19.3	20.1	20	19.8
Ge	1.1	1.3	0.8	1.2	1.2	1.2	0.9	1	1.2	0.8	1.3	1.1	1.3	1	1.3	0.9	1	1
La	34.09	25.62	29.47	21.04	28.41	23.23	23.56	25.62	16.71	15.02	15.44	20.76	14.11	8.13	7.59	11.98	12.25	9.39
Ce	63.82	47.65	56.74	39.03	55.44	45.77	47.33	51.53	32.57	32.76	41.45	39.88	33.26	20.73	15.64	25.76	24.87	18.43
Pr	6.59	5.08	5.94	4.25	6.09	4.85	5.38	5.60	3.65	3.49	3.44	4.29	3.24	2.06	2.04	2.70	2.84	2.18
Nd	25.18	19.24	23.10	15.35	21.33	18.15	21.21	21.37	13.69	13.94	14.07	16.66	13.41	8.51	8.31	10.97	11.18	8.91
Sm	4.92	4.15	4.56	3.20	4.04	3.71	4.61	4.43	3.22	3.43	3.35	3.84	3.12	2.27	2.12	2.57	2.58	2.05
Eu	1.33	0.99	1.18	0.95	1.43	1.02	1.11	1.19	0.94	0.94	0.86	0.87	0.83	0.61	0.60	0.73	0.70	0.58
Tb	0.45	0.39	0.40	0.33	0.41	0.35	0.44	0.35	0.32	0.34	0.32	0.32	0.27	0.20	0.20	0.25	0.22	0.18
Gd	3.75	3.07	3.15	2.32	3.11	2.83	3.17	2.86	2.22	2.51	2.26	2.61	2.24	1.70	1.55	1.90	1.80	1.39
Dy	2.37	2.20	2.21	1.51	2.10	1.98	2.31	1.60	2.19	1.77	1.70	1.65	1.31	1.02	1.07	1.24	1.25	0.91
Ho	0.42	0.39	0.37	0.24	0.33	0.36	0.38	0.26	0.41	0.31	0.30	0.29	0.21	0.21	0.21	0.21	0.21	0.17
Er	0.97	1.01	0.90	0.60	1.02	0.83	1.03	0.66	1.24	0.85	0.80	0.75	0.59	0.47	0.57	0.57	0.51	0.44
Tm	0.12	0.11	0.13	0.07	0.14	0.14	0.13	0.09	0.19	0.12	0.12	0.10	0.08	0.07	0.08	0.08	0.08	0.07
Yb	0.86	0.64	0.84	0.38	0.89	0.71	0.75	0.60	1.23	0.76	0.58	0.68	0.44	0.55	0.50	0.58	0.60	0.41
Lu	0.10	0.09	0.10	0.06	0.11	0.10	0.11	0.08	0.17	0.09	0.09	0.08	0.07	0.07	0.06	0.07	0.07	0.05
Rb/Sr	0.128	0.177	0.132	0.217	0.121	0.182	0.117	0.102	0.191	0.158	0.158	0.179	0.203	0.247	0.125	0.135	0.138	0.156
Nd/Th	1.657	1.644	1.650	1.668	1.720	1.621	2.001	1.842	1.538	1.340	1.497	1.666	1.507	1.051	0.649	0.850	0.947	0.810
(La/Yb)N	28.54	28.60	25.05	39.93	22.78	23.38	22.41	30.55	9.75	14.23	19.06	21.89	23.18	10.56	10.86	14.85	14.77	16.30
YbN	5.04	3.78	4.96	2.22	5.26	4.19	4.44	3.54	7.23	4.45	3.42	4.00	2.57	3.25	2.95	3.40	3.50	2.43
Eu/Eu*	0.91	0.81	0.91	1.02	1.18	0.92	0.84	0.96	1.02	0.93	0.90	0.79	0.91	0.91	0.97	0.97	0.94	1.00
$^{87}Sr/^{86}Sr$	).7086	0.7083	0.7086	0.7093	0.7067	0.7107	0.7072		0.7095		0.7080	0.7086	0.7089		0.7074			0.7081
$(^{87}Sr/^{86}Sr)_i$	).7052	0.7053	0.7058	0.7056	0.7042	0.7060	0.7046		0.7055		0.7046	0.7047	0.7050		0.7045			0.7051
T_{Zr} (C°)	918	891	909	894	899	886	893	890	873	878	875	876	863	849	848	847	853	853

TABLE II. Trace element data (ppm) of STG and BG zircons (Cameca IMS 1280)

Sample	Age		Pb	Th	U	Th/U	Y	Hf	La	Ce	Pr	Nd	Sm	Eu	Gd	Dy	Er	Yb	Ti	T_{Zr} corrected
	(Ma)	2σ	(ppm)	(ppm)	(ppm)		(ppm)	(ppm)	(ppm)	(ppm)	(ppm)	(ppm)	(ppm)	(ppm)	(ppm)	(ppm)	(ppm)	(ppm)	(ppm)	(ºC)
BG-Z13	2514	48	164.01	180.67	746.59	0.24	413.6	9712.2	15.7	22.9	29.4	33.2	72.6	47.3	181.4	212.7	379.2	709.1	24.56	879
BG-Z2	1878-1857	56-56	141.06	100.95	394.99	0.26	964.4	10389.0	0.1	2.8	0.6	2.7	17.0	2.2	87.4	346.3	780.0	1274.8	7.62	754
BG-Z11-c	1055	39							2.3	62.6	4.7	8.7	40.7	30.6	115.4	522.3	1715.1	3503.3		
BG-Z10	858	32	77.46	498.66	1097.41	0.45	1638.9	9141.6	81.4	75.9	158.7	187.0	417.7	252.5	573.6	851.2	1653.9	3336.4	34.48	921
BG-Z17-c	677	29	11.93	34.63	114.55	0.30	910.5	9801.1	0.3	3.6	0.6	1.7	9.2	5.7	39.0	212.0	996.3	3300.3	19.75	853
BG-Z12	600	22	44.92	301.31	434.50	0.69	1114.8	8436.3	0.0	21.8	1.0	4.1	27.6	7.0	117.3	438.2	1056.1	1936.5	9.69	777
BG-Z4-c	589	23	39.11	3.60	400.10	0.01	201.8	7736.3	0.3	3.5	0.2	0.2	1.2	3.1	7.9	59.2	204.8	518.6	3.37	681
BG-Z15-c	583	22							0.2	17.6	0.8	2.7	15.1	5.0	72.7	282.8	716.2	1383.6		
STG-r	493	19	23.00	241.69	396.73	0.61	3145.7	7584.5	1.0	15.1	1.2	3.1	19.9	2.2	95.0	438.8	995.8	1637.2	10.14	875
STG-c	465	17	14.05	150.39	234.46	0.64	1075.1	7218.1	47.2	98.3	28.9	27.5	82.4	4.4	327.4	1176.1	2608.9	3579.0	3.46	759
BG-Z18-r1	462	18	24.15	110.11	305.21	0.36	1599.8	9236.6	0.0	3.2	0.7	3.5	24.8	1.6	161.4	655.8	1454.4	2328.1	13.63	911
BG-Z9	434	19	8.49	114.95	113.86	1.01	2531.7	8621.9	0.2	5.9	4.4	17.1	100.9	4.8	357.5	1024.3	2001.7	2828.6	23.66	985
BG-Z16	357	15	239.63	776.77	3891.18	0.20	1891.8	8689.7	26.4	71.2	79.7	113.4	253.2	181.3	320.0	671.4	1703.7	3360.3	16.96	
BG-Z15-r	338	15							0.1	19.3	0.6	2.0	12.7	3.8	51.7	238.2	689.2	1360.4		
BG-Z4-r	331	15	57.16	28.98	893.55	0.03	240.8	9047.5	0.5	0.3	0.4	0.4	1.5	2.8	9.4	75.9	124.6	181.1	2.17	
BG-Z11-r	329	13							30.5	130.6	81.6	74.5	81.0	61.2	133.7	312.2	825.2	1641.2		
BG-Z17-r	319	14	57.87	308.09	1878.02	0.16	892.8	9952.5	12.0	31.5	26.4	29.4	57.2	58.6	109.3	250.8	752.2	1787.3	11.17	
BG-Z5	309	12	116.88	257.09	553.39	0.46	1007.3	7733.1	26.3	37.5	50.6	59.7	137.5	92.3	201.8	403.6	898.0	1733.5	25.87	